International Conference and Utility Exhibition 2014 on Green Energy for Sustainable Development (ICUE 2014)
Jomtien Palm Beach Hotel and Resort, Pattaya City, Thailand, 19-21 March 2014

Design and Simulation of High Efficiency Counter-Rotating Vertical Axis Wind Turbine Arrays

P. Chaitanya Sai[1], Richa S. Yadav[1], R. Nihar Raj [1]and G.R.K. Gupta[1]

Abstract-- **Technology to abstract energy from the wind using Vertical Axis Wind Turbines (VAWTs) has rarely been adopted for large scale power production, owing to low power coefficient of the individual turbines, as compared to Horizontal Axis Wind Turbines (HAWTs). In the last few years, much research has been done to make VAWTs more economical and efficient to increase power generated per turbine. But besides improving coefficient of power through design changes, research now focuses on maximizing power generated per unit area. Arranging VAWTs in specific layouts of Counter Rotating Arrays can enhance power production in low wind speed areas and thus increase the W. This paper analyses Counter Rotating VAWT Arrays in terms of coefficient of power and power density and further compares efficiencies in various arrangements. The effect of angle of attack on the performance of the array has also been studied further explaining the effects of arrangements on Wind Farm Power Density as well as the Total Wind Farm Power.**

Index Terms-- **Counter rotating turbines, Vertical axis wind turbine (VAWT) arrays, CFD, FLUENT, Gambit.**

I. Nomenclature

HAWT	Horizontal Axis Wind Turbine
VAWT	Vertical Axis Wind Turbine
C_p	Power Coefficient
P	Turbine Power Generated, W
a, b, c, d	Turbine Spacing, m
D	Turbine Diameter, m
C_d	Coefficient of Drag
D	Diameter of cylinder, m
U_∞	Free Stream Velocity, ms^{-1}
ρ	Density, $kg.m^{-3}$
α	Angle of attack, degrees
Suffixes:	
d	Drag
l	Lift
p	Power
max	Maximum

[1]Department of Mechanical Engineering National Institute of Technology Warangal - India

II. Introduction

For any wind farm, it is crucial to estimate how much power the farm can produce for a given wind inflow. But in the process of extracting kinetic energy, the wind turbines modify the structure of the wind flow by creating small turbulence structures and by reducing the wind velocity substantially. Therefore in any wind farm the turbines are subjected to a mixed type flow, which in part is undisturbed or uniform and in part influenced by the wake from the upstream turbines. The downstream wind turbines, as a consequence, observe a wind inflow modified both in terms of mean velocity and turbulence, producing lesser power as compared to an isolated turbine [1]. To avoid these wind and power fluctuations as well as to reduce structural vibrations and fatigue loads, wind turbines are always spaced far apart occupying large areas of land, as seen in both on-shore and off-shore farms.

To maintain 90% of the performance of isolated HAWTs, the turbines in a HAWT farm must be spaced 3–5 turbine diameters apart in the cross-wind direction and 6–10 diameters apart in the downwind direction. So even if an isolated HAWT has higher efficiency, its efficiency per unit area is lesser [2]. Also a yaw control mechanism is necessary for directional control as the turbine has to face the direction of the wind to be effective. Due to the large size of HAWT, complexity of design, maintenance and the cost of huge land area, the capital cost of a HAWT farm is very high despite which the wind farm power density is only 2 to 3 W/m^2.

However, in the case of directionally independent VAWT rotors, a mutual coupling effect exists between rotors if they are placed such that they counter rotate with respect to each other. Thus they produce positive interactions which can considerably improve the power performance of VAWTs [3]. When two counter rotating turbines are placed side by side then the flow induced by each turbine is oriented in the same direction, resulting in reduced turbulence and vortex shedding. The directionality facilitates the turbines to extract energy from adjacent wakes, resulting in higher power coefficient per turbine. Also turbulence in wake decreases, and hence the energy dissipation is reduced; therefore more wind energy can be abstracted by the downwind turbines as compared to two turbines rotating in the same direction, improving the overall power produced by the wind farm [4], [5].

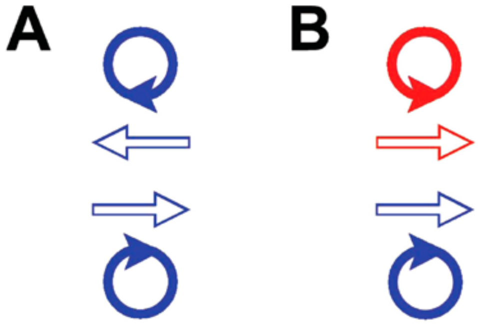

FIG. 1: (A) UNI DIRECTIONAL ROTATING VAWTS AND (B) COUNTER ROTATING VAWTS [6]

In the past, the field of VAWT arrays with counter rotating turbines has been rarely explored. The present project aims at investigating the inter-turbine spacing effects of VAWT arrays for enhanced power output of the wind turbine plants by the use of counter-rotating VAWTs. Further, it is proposed to carry out the simulation studies using FLUENT 12.0 using the standard k-ε turbulence model considering the fact that the results are very close to the experimental results.

III. METHODOLOGY

If VAWTs have been be modelled as rotating cylinders converting the problem statement into the analysis of flow over an array of rotating cylinders. The flow has been assumed to be two dimensional (neglecting the influence of the three dimensional turbulence effects) such that the flow satisfies the boundary conditions of the undisturbed wind velocity far upstream, and no-through and no-slip conditions at the rotor boundaries[7]. In order to decide on the turbulence model to be used, to obtain results close to experimental values, analysis of the flow over a single non rotating cylinder in both steady and unsteady flow conditions was done. The flow over various arrangements of rotating cylinders was done, finally arriving at the best possible arrangement of twelve rotating cylinders, to finally calculate the Power Density and the Power generated in the array. The power coefficient is obtained as,

$$C_p = P/\left(0.5\ \rho A V_w^3\right) \quad (1)$$

The maximum power output from a single turbine can be obtained as,

$$P_{max} = C_{pmax} \times 0.5\ \rho A V_w^3 \quad (2)$$

The maximum value of C_P was obtained as,

$$C_{pmax} = (4/27)\ C_d \quad (3)$$

$$P_{max} = (4/27)\ C_d \times 0.5\ \rho A V_w^3 \quad (4)$$

The simulations were carried out using commercial computational fluid dynamics code ANSYS FLUENT 12.0 and the mesh files for this were generated using GAMBIT 2.2.30. The computational domain consists of an upstream of 13 times the diameter to downstream of 40 times the diameter of the cylinder and 13 times the diameter on each cross-stream direction. The diameter is considered to be 1.5m in each case.

The quintessential points of reliability of CFD prediction in static conditions are:

- Capturing the boundary layer
- Establishing grid independency
- Closeness of the prediction with the theoretical or established results [8], [9].

In every solution, the above conditions were verified and then accepted.

IV. GRID REFINEMENT

A systematic method of refining a computational grid for the numerical simulation of flow over a no rotating single cylinder at $R_e = 1.0268 \times 10^5$ is done by construction of computational meshes based on reasonable estimates of cell size and the closeness of theoretical and simulated values. The appropriateness of the grid for the study is defined by the grid convergence index, defined as,

$$Gridconvergenceindex = \frac{Cdtheoretical - Cdsimulated}{Cdtheoretical} \times 100 \quad (5)$$

TABLE 1
GRID STUDY FOR STEADY FLOW OVER NON-ROTATING CYLINDER

Si. No.	Elements	C_d Simulated	C_d Theoretical	Grid Convergence Index
1	2544	0.9337	1.0	6.63
2	9081	0.9457	1.0	5.43
3	30859	0.9962	1.0	0.381
4	34059	0.9970	1.0	0.3

After the grid refinement study, the comparison between the simulated values calculated from the finest grid with 34059 elements (table 1) and the theoretical values indicated that it the finest grid was appropriate to be used in the further analysis.

V. RESULTS AND DISCUSSION

The simulations are carried out for unsteady flow conditions as this is close to the actual flow over turbines ($R_e = 1.026 \times 10^5$).

A. Flow over Tandem Arrangement:

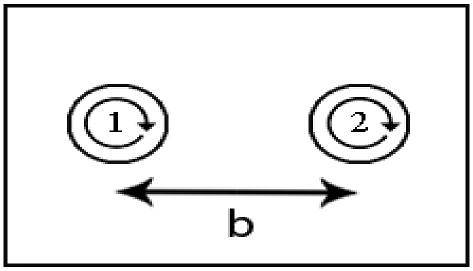

FIG. 2: TANDEM ARRANGEMENT OF ROTATING CYLINDERS

Free stream velocity $U_\infty = 3\ ms^{-1}$

The present case deals with the calculation of average coefficient of drag and visualization of flow over a pair of rotating cylinders in tandem arrangement (Fig 2). The distance between the two cylinders, 'b' is varied from 5D to 11D and C_d of cylinders 1 and 2 are obtained and the average C_d is calculated (table 2)

TABLE 2
CD VALUES FOR FLOW OVER TANDEM ARRANGEMENT OF ROTATING CYLINDERS

Distance	C_d - cyl1	C_d - cyl2	C_d average
5d	0.88197	0.48666	0.69341
6d	0.91025	0.51499	0.71262
7d	0.89049	0.56148	0.72596
8d	0.9352	0.57155	0.75338
9d	0.9385	0.61519	0.77684
10d	**0.94364**	**0.62594**	**0.78479**
11d	0.94626	0.61912	0.78269

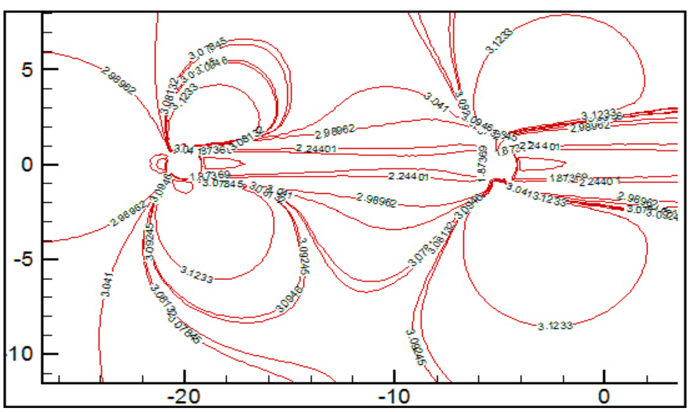

Fig. 3: Velocity contour plot of flow over tandem arrangement of rotating cylinders

Evaluation of results and inferences:

It is observed that the maximum value of average C_d is obtained at a distance of 10D between the cylinders (table 2). Hence, this distance is used for maximizing efficiency involving tandem arrangement of the cylinders.

Horizontal distance between the cylinders (b) = 10D = 15 m

B. Flow over Transverse Arrangement:

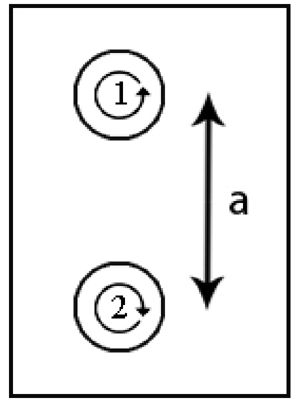

FIG. 4: TRANSVERSE ARRANGEMENT OF A PAIR OF ROTATING CYLINDERS

Free stream velocity $U_\infty = 3\ ms^{-1}$

The present case deals with the calculation of average coefficient of drag and visualization of flow over a pair of rotating cylinders in transverse arrangement (Fig 4). The distance between the two cylinders, 'a' is varied from 2D to 6D and C_d of cylinders 1 and 2 are obtained and the average C_d is calculated (table 3).

TABLE 3
C_D VALUES FOR FLOW OVER TRANSVERSE ARRANGEMENT OF A PAIR OF ROTATING CYLINDERS

Transverse distance	C_d-cyl1	C_d-cyl2	C_d average
2d	**1.1609**	**1.1636**	**1.16225**
3d	1.0515	1.0618	1.05665
4d	1.0087	1.0237	1.0162
5d	1.0032	0.9878	0.9955
6d	1.0006	1.0058	1.0032

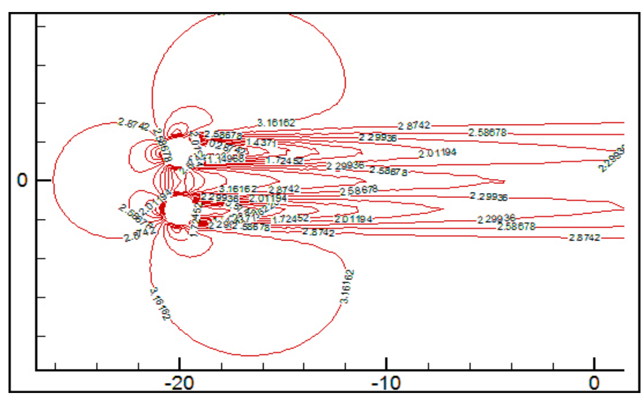

Fig. 5: Velocity contour plot of flow over transverse arrangement of a pair of rotating cylinders

Evaluation of results and inferences:

It is observed that the maximum value of average C_d is obtained at a distance of 2D between the cylinders (table 3). Hence, this distance is used for maximizing efficiency involving transverse arrangement of the cylinders.

Vertical distance between the cylinders (b) = 2D = 3 m

C. Flow over Three Rotating Cylinders Placed in a Staggered Pattern

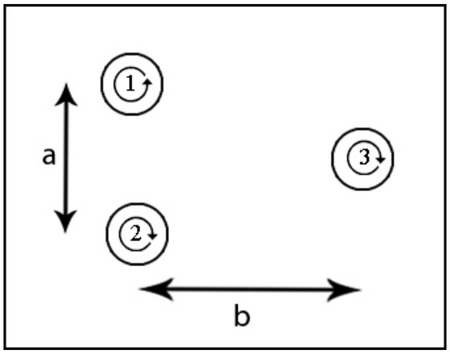

FIG. 6: STAGGERED ARRANGEMENT OF 3 ROTATING CYLINDERS (UNIT CELL)

This staggered arrangement of three rotating cylinders is used further in this report and will be referred to as the "unit cell" (Fig 6). This is owing to the fact that it has been observed that a staggered pattern results in a better C_d values compared to inline arrangement for the same number of cylinders (Table 4).

Free stream velocity $U_\infty = 3\ ms^{-1}$

Vertical distance between the cylinders (a) = 4D = 6 m

The present case deals with the calculation of average coefficient of drag and visualization of flow over the "unit cell" arrangement of rotating cylinders. The distance between the two cylinders, 'b' is varied from 8D to 12D, the C_d of cylinders 1, 2 and 3 are obtained and the average C_d is calculated.

TABLE 4
C_D VALUES FOR FLOW OVER STAGGERED ARRANGEMENT OF 3 ROTATING CYLINDERS

Distance	C_d1	C_d2	C_d3	C_d average
d	1.0064	1.0064	0.9209	0.9779
9d	**1.017**	**1.017**	**0.91239**	**0.98213**
10d	0.996	1.0006	0.88302	0.95987
11d	0.99554	1.0041	0.89847	0.96603
12d	0.99691	1.0053	0.89168	0.96463

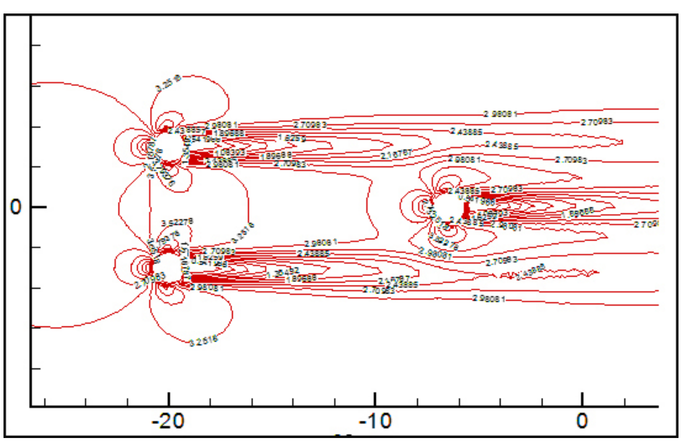

FIG. 7: VELOCITY CONTOUR PLOT OF FLOW OVER STAGGERED ARRANGEMENT OF 3 ROTATING CYLINDERS

Evaluation of results and inferences:

It is observed that the maximum value of average C_d is obtained at a horizontal distance of 9D between the cylinders (table 4). Hence, this distance is used as the horizontal distance in the unit cell.

Horizontal distance between the cylinders (b) = 9D = 13.5 m

D. Flow over Transverse Arrangement of Two Cylinders for Optimum Interference

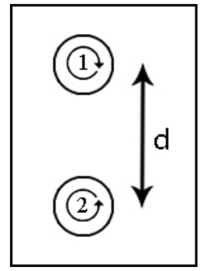

FIG.8: TRANSVERSE ARRANGEMENT OF 2 ROTATING CYLINDERS FOR OPTIMUM INTERFERENCE

Free stream velocity $U_\infty = 3\ ms^{-1}$

The present case deals with the calculation of average coefficient of drag and visualization of flow over a transverse arrangement of rotating cylinders (Fig 8). The distance between the two cylinders "d" is varied from 4D to 9D and C_d of cylinders 1 and 2 are obtained and the average C_d is calculated (table 5). Here, the two cylinders must have minimum effect on each other. This condition is met with if the average C_d of the cylinders is as close as possible to the C_d of a single rotating cylinder. The parameter used for judging this criterion is the "Percentage C_d difference" denoted by $\%C_d$ and defined as

$$\%C_d = (C_{davg} - C_{ds}) \times 100 / C_{ds} \qquad (6)$$

C_{ds} is C_d of a single rotating cylinder and has a value of 1.07.

TABLE 5:
C_D VALUES FOR FLOW OVER TRANSVERSE ARRANGEMENT OF 2 ROTATING CYLINDERS FOR OPTIMUM INTERFERENCE

Transverse distance	C_d1	C_d2	C_d average	$\%C_d$
9d	0.99604	0.98959	0.99281	0.91682
8d	0.9935	1.0002	0.99685	2.5514
7d	**0.97659**	**0.97659**	**0.97659**	**3.14299**
6d	0.96058	0.97602	0.9683	10.2439
5d	0.9774	0.9699	0.97365	10.40654
4d	0.99545	0.97085	0.98315	11.85514

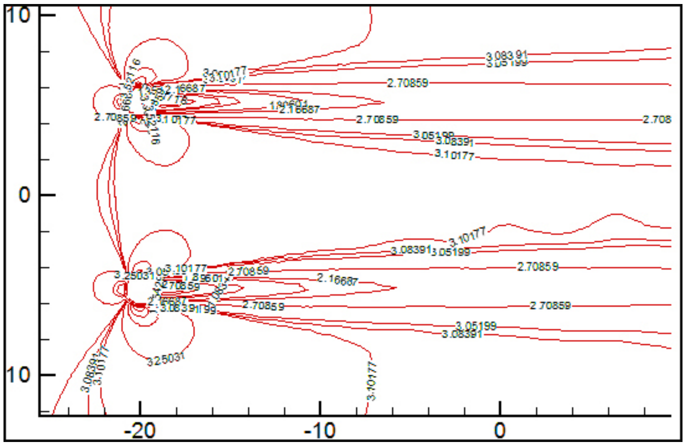

FIG. 9: VELOCITY CONTOUR PLOT FOR FLOW OVER TRANSVERSE ARRANGEMENT OF 2 ROTATING CYLINDERS FOR OPTIMUM INTERFERENCE

Evaluation of results and inferences:

It is observed that the value of %C_d is very less for a transverse distance of 9D. As the distance decreases to 4D, %C_d increases. It is to be noted that the increase in %C_d is drastic as the distance decreases from 7D to 6D. Hence, to strike a balance between the area occupied by the VAWT array and the no mutual effect condition, a transverse distance of 7D is chosen as the optimum distance to achieve no mutual effect (table 6.11)

Vertical distance between the cylinders for optimum interference (d) = 7d = 10.5 m

E. Flow over Six Rotating Cylinders Placed in a Staggered Pattern

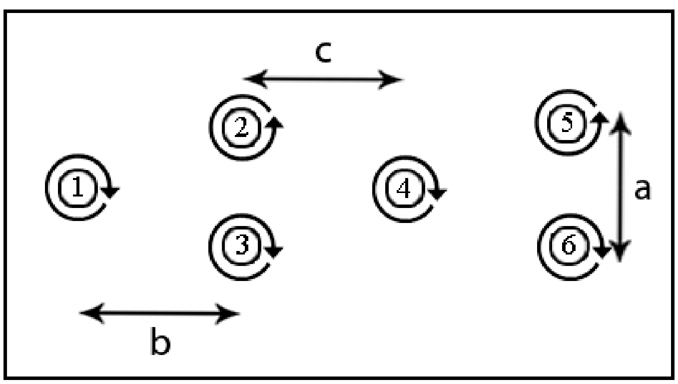

FIG. 10: STAGGERED ARRANGEMENT OF 6 ROTATING CYLINDERS

Free stream velocity $U_\infty = 3\ ms^{-1}$
Horizontal distance between the cylinders (b) = 9D = 13.5 m
Vertical distance between the cylinders (a) = 4D = 6 m

The present case deals with the calculation of average coefficient of drag and visualization of flow over two unit cells placed in a tandem arrangement (Fig 10). The distance between the two cells, 'c' is varied from 7D to 11D, C_d of cylinders 1 to 6 are obtained and the average C_d is calculated (table 6).

TABLE 6
CD VALUES FOR FLOW OVER STAGGERED ARRANGEMENT OF 6 ROTATING CYLINDERS

c	C_d1	C_d2	C_d3	C_d4	C_d5	C_d6	C_d avg
7d	0.8968	0.9752	0.9675	0.6556	0.7304	0.7347	0.8267
8d	0.8934	0.9755	0.9639	0.6894	0.7450	0.7364	0.8339
9d	0.9079	0.9758	0.9773	0.6752	0.7369	0.7324	0.8343
10d	**0.9133**	**0.9711**	**0.9591**	**0.7053**	**0.7501**	**0.7324**	**0.8385**
11d	0.9185	0.9732	0.9627	0.6844	0.7410	0.7395	0.83539

It is observed that the maximum value of average C_d is obtained at a horizontal distance of 10D between the unit cells. Hence this distance is fixed as the optimum distance between two unit cells when they are placed in a tandem arrangement.

Horizontal distance between two patterns (c) = 10D = 15 m.

F. Flow over Six Rotating Cylinders Placed in an Inline Pattern

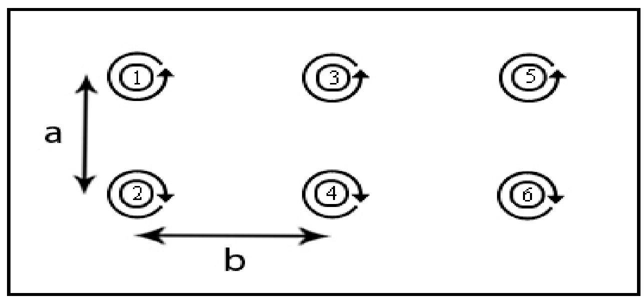

FIG. 11: INLINE PATTERN OF 6 ROTATING CYLINDERS

Free stream velocity $U_\infty = 3\ ms^{-1}$
Horizontal distance between the cylinders (b) = 7D = 10.5 m
Vertical distance between the cylinders (a) = 2D = 3 m

The present case deals with the calculation of average coefficient of drag and visualization of flow over an inline arrangement of VAWTs (Fig 11). The C_d of cylinders 1 to 6 are obtained and the average C_d of the array is calculated. This is later compared with the average C_d of the staggered pattern and the 12 cylinder array (Table 7).

TABLE 7
CD VALUES FOR FLOW OVER INLINE ARRANGEMENT OF 6 ROTATING CYLINDERS

Inline array	2d X 7d
Cd1	1.101
Cd2	1.0855

Cd3	0.69907
Cd4	0.67711
Cd5	0.5594
Cd6	0.54211
Cd average	0.77736

This is the most widely used array in small scale VAWT farms. Here, the turbines can be packed closer together and hence resulting in a high value of wind farm power density.

VI. Optimum 12 Cylinder Staggered Array

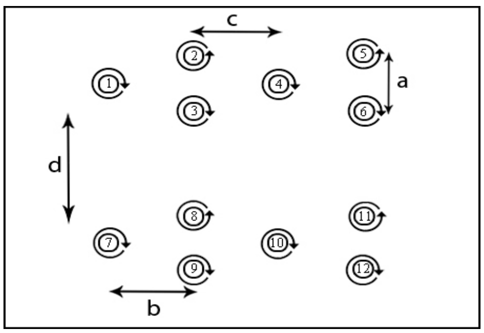

Fig. 12: Staggered array of 12 rotating cylinders

The optimum values from the previously analyzed individual configurations are used to obtain an efficient array in terms of its coefficient of power. In order to reduce the computational load and increase the computational time, a single staggered array comprising of two unit cells is used (Fig 12). By applying the symmetry condition at the lower boundary, results analogous to a twelve cylinder array were achieved. The 12 cylinder staggered array has the following dimensions:

Vertical distance between the cylinders (a) = 4D = 6 m
Horizontal distance between the cylinders (b) = 9D = 13.5 m
Distance between two horizontal patterns (c) = 10D = 15 m
Distance between two vertical patterns (d) = 7D = 10.5 m

A. Effect of Angle of Attack on C_d Average

The present case deals with the calculation of average coefficient of drag and visualization of flow over the 12 cylinder array of rotating cylinders. The varying parameter in this case is the angle of attack measured with respect to the horizontal (table 6.14).
Free stream velocity $U_\infty = 3\ ms^{-1}$

TABLE 8
CD VALUES FOR FREE STREAM VELOCITY OF 3 MS^{-1} AND VARYING ANGLE OF ATTACK

U_∞	C_d1	C_d2	C_d3	C_d4	C_d5	C_d6	C_d Avg
0	0.9164	0.9892	0.9977	0.6855	0.7492	0.7728	0.85185
4	0.7885	0.8057	0.7753	0.5081	0.4638	0.4816	0.6372
8	0.6893	0.6872	0.6176	0.4201	0.3565	0.3425	0.51891
12.5	0.5685	0.5465	0.4354	0.3105	0.2916	0.2895	0.40703

Case 1:
Angle of attack = 0°

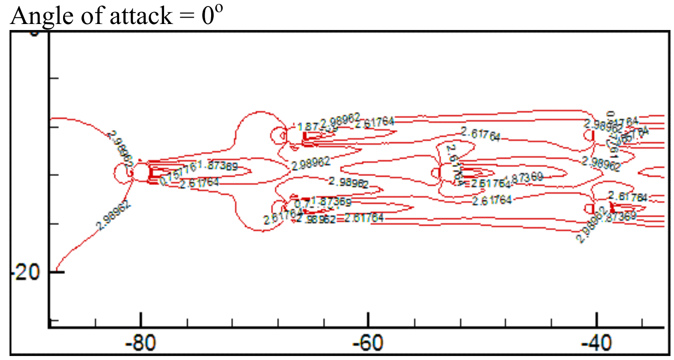

Fig. 13: Velocity contour plot of 12 cylinder staggered array with free stream velocity 3 ms^{-1} and zero angle of attack

Case 2:
Angle of attack = 4°

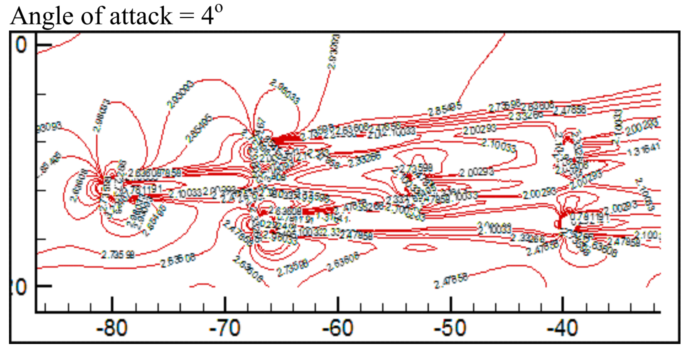

Fig. 14: Velocity contour plot of 12 cylinder staggered array with free stream velocity 3 ms^{-1} and angle of attack 4 degrees

Case 3:
Angle of attack = 8°

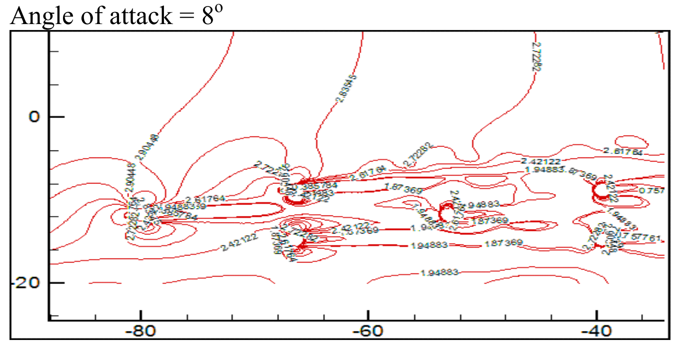

Fig. 15: Velocity contour plot of 12 cylinder staggered array with free stream velocity 3 ms^{-1} and angle of attack 8 degrees

Case 4:
Angle of attack = 12.53°

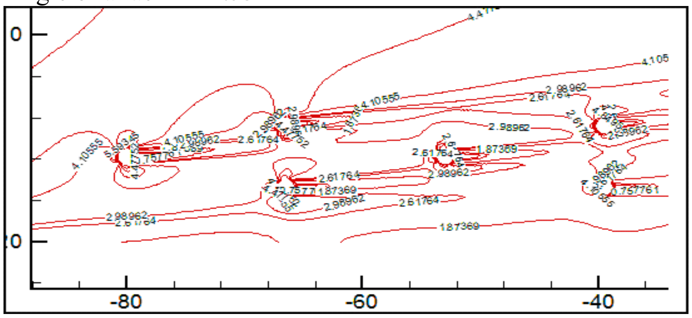

FIG. 16: VELOCITY CONTOUR PLOT OF 12 CYLINDER STAGGERED ARRAY WITH FREE STREAM VELOCITY 3 MS^{-1} AND ANGLE OF ATTACK 12.53 DEGREES

The analysis is carried out with an increasing value of angle of attack from zero, which is a direct impact, to an angle of attack of 12.53 degrees at which point the array becomes analogous to the inline array. It is observed that the average value of C_d decreases with an increase in the angle of attack, the maximum value being observed when the angle of attack is zero.

B. *Effect of Free Stream Velocity on C_d Average*

The present case deals with the calculation of average coefficient of drag and visualization of flow over the 12 cylinder array of rotating cylinders. The varying parameter in this case is the free stream velocity.
Angle of attack = 0°

TABLE 9
C_D VALUES WITH ZERO ANGLE OF ATTACK AND VARYING FREE STREAM VELOCITY

U_∞	3	4	5
Cd 1	0.9164	0.8766	0.85
Cd 2	0.9892	0.9538	0.9287
Cd 3	0.9977	0.9628	0.9386
Cd 4	0.6855	0.6704	0.659
Cd 5	0.7492	0.7459	0.7432
Cd 6	0.7728	0.7644	0.7586
Cd avg	0.8518	0.8385	0.8131

Case 1:
Free stream velocity U_∞ = 3 ms^{-1}

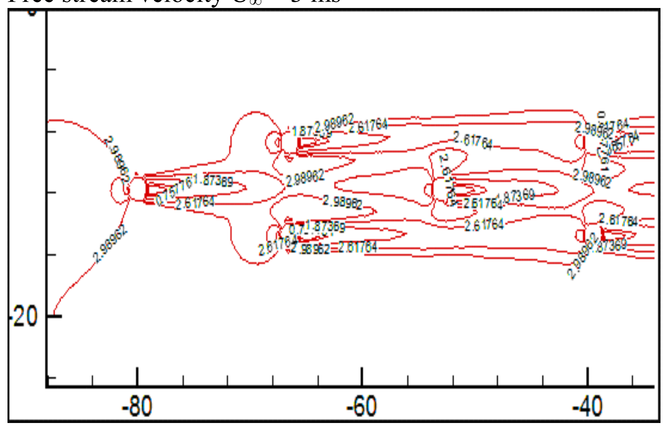

FIG. 17: VELOCITY CONTOUR PLOT OF 12 CYLINDER STAGGERED ARRAY WITH ZERO DEGREES ANGLE OF ATTACK AND FREE STREAM VELOCITY 3 MS^{-1}

Case 2:
Free stream velocity U_∞ = 4 ms^{-1}

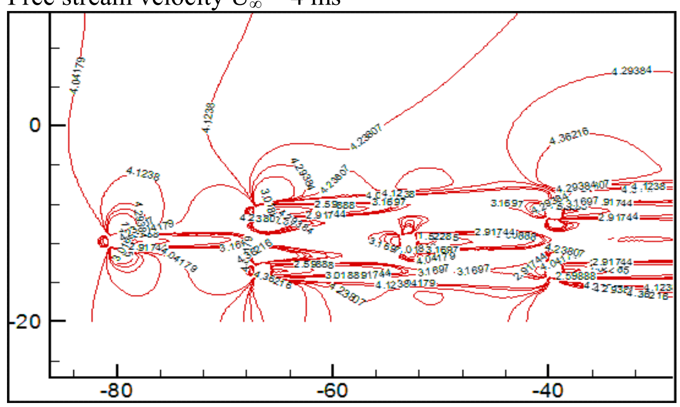

FIG. 18: VELOCITY CONTOUR PLOT OF 12 CYLINDER STAGGERED ARRAY WITH ZERO DEGREES ANGLE OF ATTACK AND FREE STREAM VELOCITY 4 MS^{-1}

Case 3:
Free stream velocity U_∞ = 5 ms^{-1}

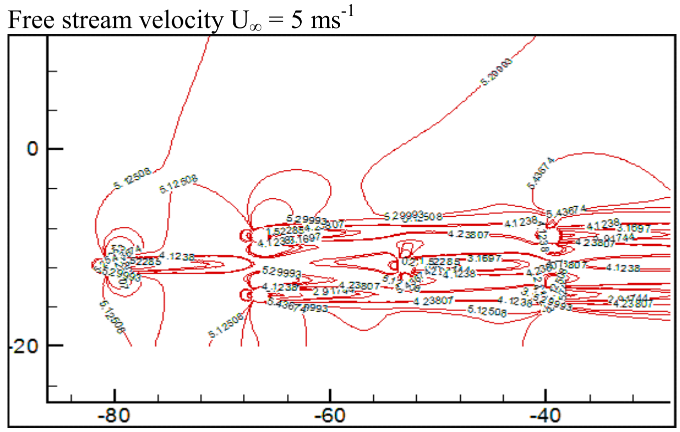

FIG. 19: VELOCITY CONTOUR PLOT OF 12 CYLINDER STAGGERED ARRAY WITH ZERO DEGREES ANGLE OF ATTACK AND FREE STREAM VELOCITY 5 MS^{-1}

The analysis is carried out with increasing value of free stream velocity from 3 ms^{-1} to 5 ms^{-1}. It is to be noted that despite the fact that the average value of C_d decreases, the overall power output from the VAWT array increases.

VII. Conclusion

By conducting the above study, we can calculate the parameters for Power in VAWTs. The power generated per cylinder in case C is higher as compared to case B due to the increased turbulence effects by the presence of 6 additional cylinders. The increased turbulence increases the power generated per cylinder by 1.59% hence proving that better results can be obtained due to increased turbulence in case of VAWTs.

TABLE 10:
CONSOLIDATED RESULTS OBTAINED FROM ALL THE ARRAYS

Array	Power generated (W)	Power density (W/m^2)	Average power generated per cylinder
Inline 6 turbines	171.409	1.6929	28.5681
Staggered 6 turbines	184.907	0.5667	30.8177
Staggered 12 turbines	375.666	0.3598	31.3054

This study also helps us understand which arrangement can be adopted as per the availability of land:

- The total power generated is high in case c owing to the fact that more turbines are present, when compared to 6 cylinders in case A & B. However the area required for such a plant would be very large and hence such arrangements are to be adopted where land is easily available for large scale power plants.
- The power density of case A is far higher owing to the fact that the area of the array is very less and hence this would be preferred in area with high land costs. Most of the arrays in urban areas and small scale wind turbine plants can adopt Inline arrangement of turbines.

VIII. References

[1]. Martin O.L. Hansen, Aerodynamics of Wind Turbines, 2nd Edition, Earthscan, 2008

[2]. Erich Hau, *Wind Turbines Fundamentals, Technologies, Application and Economics*, 2nd Edition, Springer Publications, 2006.

[3]. Robert W. Whittlesey, Sebastian Liska and John O Dabiri, Fish schooling as a basis for vertical axis wind turbine farm design, Bioinspiration & Biomimetics Volume 5, Issue 3, Number 035005, 2010.

[4]. P.R. Schatzle, Paul C. Klimas and H.R. Spahr, Aerodynamic Interference Between Two Darrieus Wind Turbines, Journal of Energy, Volume 5, Number 2, pp. 84-88, 1981.

[5]. R. Ganesh Rajagopalan, Paul C. Klimas and Ted L. Ricker, Aerodynamic interference of vertical axis wind turbines. Journal of Propulsion and Power, Volume 6: 645–653, 1990.

[6]. John O. Dabiri, Potential Order-Of-Magnitude Enhancement of Wind Farm Power Density via Counter-Rotating Vertical-Axis Wind Turbine Array, Journal of Renewable and Sustainable Energy, Volume 3, Issue 4, Number 043104, 2011.

[7]. D. V. Patil And K. N. Lakshmisha, "Two-Dimensional Flow Past Circular Cylinders Using Finite Volume Lattice Boltzmann Formulation", International Journal For Numerical Methods In Fluids, Volume 69:1149–1164, 2011

[8]. Jiyuan Tu, Guan Heng Yeoh and Chaoqun Liu, *Computational Fluid Dynamics, A Practical Approach*, 1st edition, Elsevier Academic Press, 2008.

[9]. John D. Anderson Jr., Computational Fluid Dynamics, The Basics with applications, International Edition, 1995.

[10]. Ronnie R. Pedersen and Søren Leth, Modelling Of Flow Around Two Aligned Cylinders, 22nd Nordic Seminar On Computational Mechanics, 2009.

[11]. C.D. Markfort, W. Zhang and F. Porté-Agel, "Turbulent Flow And Scalar Flux Through And Over Aligned And Staggered Wind Farms", Journal of Turbulence, Volume. 13, Number. 1, p. N33, 2012.

[12]. D. Sumner, Y S. J. Price and M. P. Paidoussis, "Flow-Pattern Identification for Two Staggered Circular Cylinders In Cross-Flow", Journal of Fluid Mechanics, Volume 411, pp. 263-303, Cambridge University Press, 2000.

[13]. M. M. Zdravkovich, The Effects Of Interference Between Circular Cylinders In Cross Flow, Journal Of Fluids And Structures, 1987.

IX. Biographies

G.R.K. Gupta was born in Vizianagaram, India on 19 May, 1959. He did his masters course from IISC Bangalore. His paper "Tracking system for SPV systems at places in temperate zone" was presented at Proc. ISES forum, Mexico, 2000. He is currently working as an Associate Professor in Mechanical Engineering Department of National Institute of Technology, Warangal. He is guiding the current work towards the completion of Bachelor's degree of the aforementioned students.

P. Chaitanya Sai was born in Machilipatnam, India on 23 October, 1991. Both his parents being teachers, it was his second nature to be interested in scientific research. He is pursuing his bachelor's degree from National Institute of Technology, Warangal in the field of Mechanical Engineering. His field of interest is Thermal Sciences in general, and Heat Transfer, Computational Methods in particular. Chaitanya Sai also co-authored a paper "Efficiency Improvement of Solar Panels using Active Cooling Techniques" in EEIC conference, 2012. The current work is towards the completion of his Bachelor's degree.

Richa S. Yadav was born in Gwalior, Madhya Pradesh, India on 27 April, 1991. She is pursuing her bachelor's degree in the field of Mechanical Engineering from National Institute of Technology, Warangal. The current work is towards the completion of her Bachelor's degree.

Nihar Raj R. was born in Hyderabad, India on 27 September, 1991. He is pursuing his bachelor's degree in the field of Mechanical Engineering from National Institute of Technology, Warangal. He is the captain for the college BAJA team which represents the college in the national level competition SAE BAJA. The current work is towards the completion of his Bachelor's degree.